



**“Search for isotopic symmetry violation
in strong interactions at high p_T region
and the tagging stations for SPD”**

Shimanskiy S.S. (JINR)

From the inclusive experiments to the correlations and the exclusive experiments

“New directions in science are launched by new tools much more often than by new concepts.

The effect of a concept-driven revolution is to explain old things in new ways.

The effect of a tool-driven revolution is to discover new things that have to be explained”

From Freeman Dyson ‘Imagined Worlds’



1. Diquark properties.
2. Nature of the spin effects.
3. Exotic states and **flavor universality**.
4. FSI (with s, c -quarks participation).
5. ΛN - hypernuclei.
6. Nature of CsDBM.
7. Subthreshold J/Ψ production.
8. The Deuteron spin structure.
9. np dilepton production anomaly.
- 10....



HESR - High Energy Storage Ring



- Production rate $2 \times 10^7/\text{sec}$

- $P_{\text{beam}} = 1 - 15 \text{ GeV/c}$

- $N_{\text{stored}} = 5 \times 10^{10} \bar{p}$

- Internal Target

High resolution mode

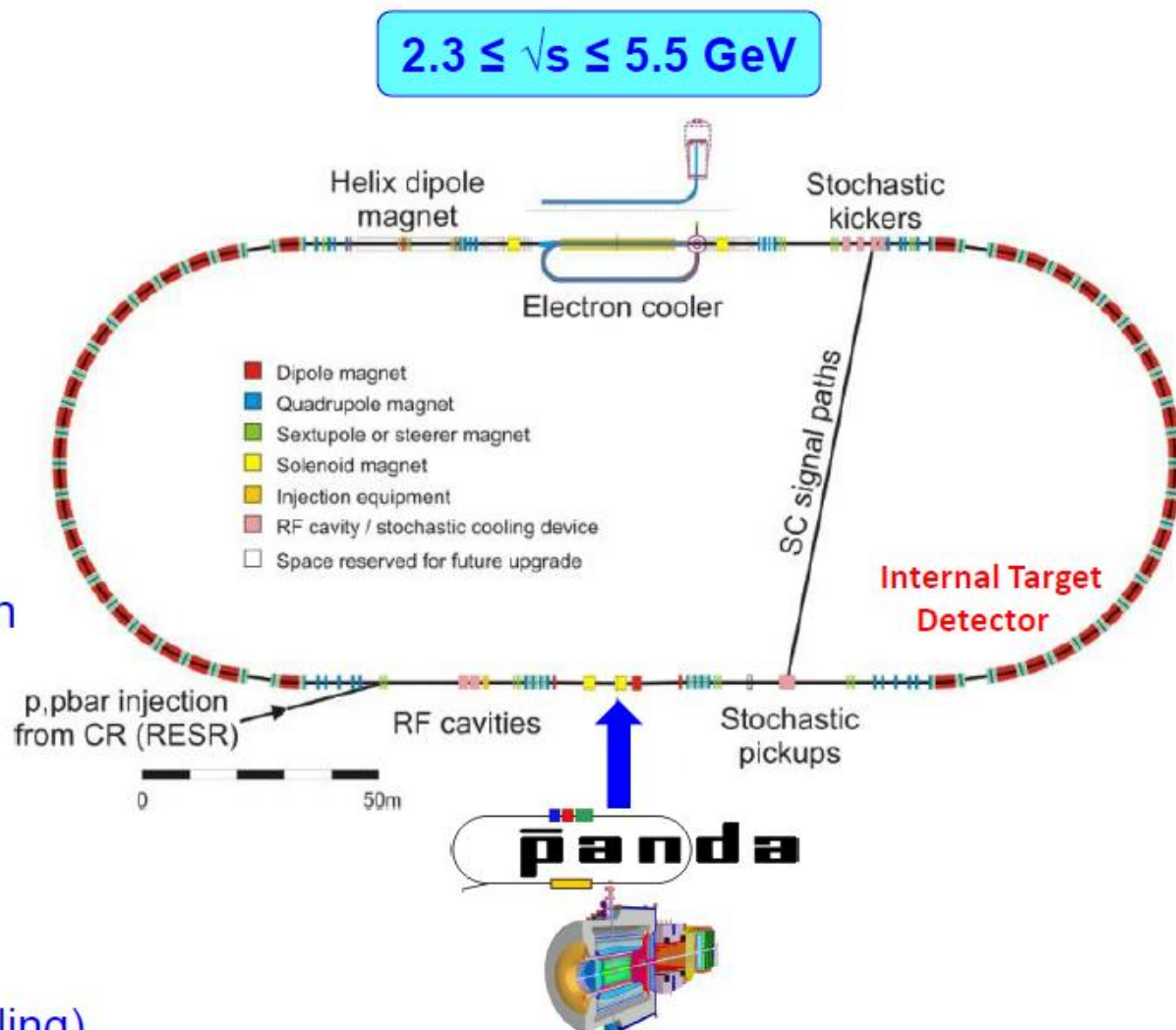
- $\delta p/p \sim 10^{-5}$ (electron cooling)

- Lumin. = $10^{31} \text{ cm}^{-2} \text{ s}^{-1}$

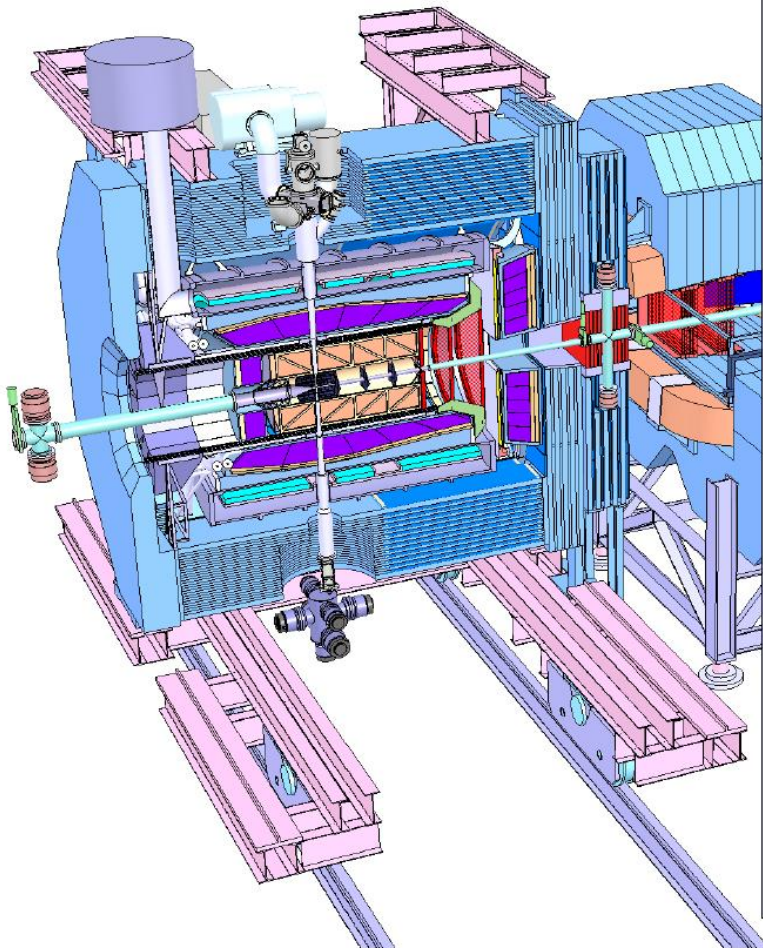
High luminosity mode

- Lumin. = $2 \times 10^{32} \text{ cm}^{-2} \text{ s}^{-1}$

- $\delta p/p \sim 10^{-4}$ (stochastic cooling)



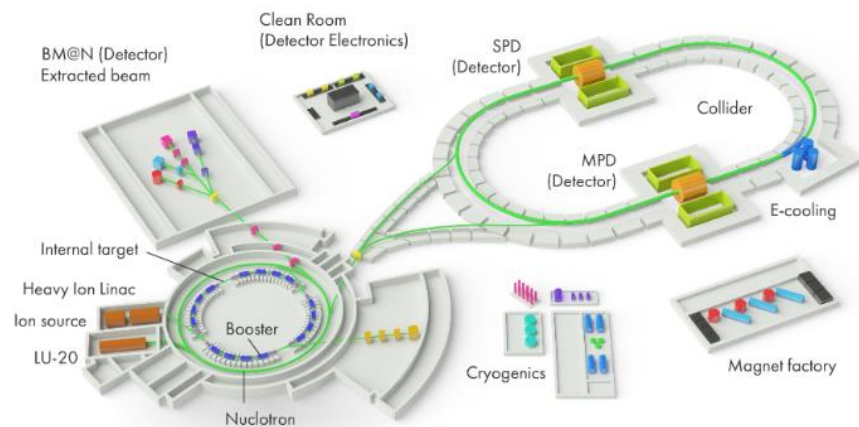
PANDA Spectrometer



Detector requirements:

- 4π acceptance
- High rate capability:
 $2 \times 10^7 \text{ s}^{-1}$ interactions
- Efficient event selection
- Continuous acquisition
- Momentum resolution $\sim 1\%$
- Vertex info for D, K_s^0 , Y
($c\tau = 317 \mu\text{m}$ for D^\pm)
- Good tracking
- Good PID (γ , e, μ , π , K, p)
- Cherenkov, ToF, dE/dx
- γ -detection MeV – 15 GeV
- Crystal Calorimeter

Requirements for the SPD



- close to 4π geometrical acceptance;
- high-precision ($\sim 50 \mu\text{m}$) and fast vertex detector;
- high-precision ($\sim 100 \mu\text{m}$) and fast tracker,
- good particle ID capabilities;
- efficient muon range system,
- good electromagnetic calorimeter,
- low material budget over the track paths,
- trigger and DAQ system able to cope with event rates at luminosity of $10^{32} (\text{cm.s})^{-1}$,
- modularity and easy access to the detector elements, that makes possible further reconfiguration and upgrade of the facility.

Main advantages

The unique beams: – wide range of kind of the beam particles (antiproton and polarization) and $\Delta p/p$ up to 10^{-5} .

The unique detectors: $\Delta\Omega \sim 4\pi$ (exclusive reactions, correlations); detection all kinds of particles; working at luminosity $\sim 10^{32} \text{ cm}^{-2} \text{ s}^{-1}$ (the rare event can be investigated); PID – close to full energy range and high momentum resolution.

Why the high p_T is needed?

The Counting Rules

Two articles in 1973 were published:

Matveev V.A., Muradyan R.M., Tavkhelidze A.N. Lett. Nuovo Cimento 7,719 (1973);

Brodsky S., Farrar G. Phys. Rev. Lett. 31,1153 (1973)

Predictions that for momentum $p_{\text{beam}} \geq 5 \text{ GeV}/c$ in any binary large-angle scattering ($\theta_{\text{cm}} > 40^\circ$) reaction at large momentum transfers $Q = \sqrt{-t}$:

$$A + B \rightarrow C + D$$

$$\frac{d\sigma}{dt}_{A+B \rightarrow C+D} \sim S^{-(n_A+n_B+n_C+n_D-2)} f\left(\frac{t}{S}\right)$$

where n_A, n_B, n_C and n_D the amounts of elementary constituents in A, B, C and D.

$$\begin{array}{ccc} s = (p_A + p_B)^2 & \text{and} & t = (p_A - p_C)^2, \\ \frac{d\sigma}{dt}_{pp \rightarrow pp} \sim S^{-10} & \text{and} & \frac{d\sigma}{dt}_{\pi p \rightarrow \pi p} \sim S^{-8} \end{array}$$

Unified description of inclusive and exclusive reactions at all momentum transfers*

R. Blankenbecler and S. J. Brodsky

$$E \frac{d\sigma}{d^3p} (A+B \rightarrow C+X) \rightarrow (p_T^2)^{-N} f\left(\frac{\mathfrak{M}^2}{s}, \frac{t}{s}\right)$$

and^{5,6}

$$\frac{d\sigma}{dt} (A+B \rightarrow C+D) \rightarrow (p_T^2)^{-N} f\left(\frac{t}{s}\right)$$

The entire kinematic range of high-energy inclusive reactions is illustrated on the Peyrou plot of Fig. 1. As usual we define

$$s = (p_A + p_B)^2, \quad t = (p_A - p_C)^2,$$

$$u = (p_B - p_C)^2, \quad \mathfrak{M}^2 = (p_A + p_B - p_C)^2,$$

and

$$\epsilon = \mathfrak{M}^2/s \cong (1 - p_{c.m.}/p_{\max}),$$

$$x_T = p_T/p_{\max}, \quad x_L = p_L/p_{\max} \cong (t-u)/s.$$

TABLE I. The expected dominant subprocesses for selected hadronic inclusive reactions at large transverse momentum. The second column lists the important exclusive processes which contribute to each inclusive cross section at $\epsilon \sim 0$. The basic subprocesses expected in the CIM, and the resulting form of the inclusive cross section $E d\sigma/d^3p \sim (p_\perp^2)^{-N} \epsilon^P$ for $p_\perp^2 \sim \infty$, $\epsilon \rightarrow 0$, and fixed $\theta_{c.m.}$ are given in the last columns. The subprocesses that have the dominant p_\perp dependence at fixed ϵ are underlined. For some particular final-state quantum numbers, the above powers of ϵ should be increased.

Inclusive process	Exclusive-limit channel	Subprocesses	$\frac{d\sigma}{d^3p/E} (\theta \sim 90^\circ)$
$M+B \rightarrow M+X$	$M+B \rightarrow M+B^* \quad (n=10)$	$\underline{M+q \rightarrow M+q}$ $\underline{q+B \rightarrow M+qq}$ $M+B \rightarrow M+B^*$	$(p_\perp^2)^{-4}\epsilon^3$ $(p_\perp^2)^{-6}\epsilon^1$ $(p_\perp^2)^{-8}\epsilon^{-1}$
$B+B \rightarrow B+X$	$B+B \rightarrow B+B^* \quad (n=12)$	$\underline{B+q \rightarrow B+q}$ $\underline{(qq)+(qq) \rightarrow B+q}$ $\underline{B+(qq) \rightarrow B+qq}$ $B+B \rightarrow B+B^*$	$(p_\perp^2)^{-6}\epsilon^3$ $(p_\perp^2)^{-6}\epsilon^3$ $(p_\perp^2)^{-8}\epsilon^1$ $(p_\perp^2)^{-10}\epsilon^{-1}$
	$B+B \rightarrow B+B^*+M^* \quad (n=14)$	$\underline{q+q \rightarrow B+\bar{q}}$ $\underline{q+(qq) \rightarrow B+M^*}$ $\underline{(qq)+B \rightarrow B+M^*+qq}$ $B+B \rightarrow B+B^*+M^*$	$(p_\perp^2)^{-4}\epsilon^7$ $(p_\perp^2)^{-6}\epsilon^5$ $(p_\perp^2)^{-10}\epsilon^1$ $(p_\perp^2)^{-12}\epsilon^{-1}$
$B+B \rightarrow M+X$	$B+B \rightarrow M+B^*+B^* \quad (n=14)$	$\underline{q+(qq) \rightarrow M+B^*}$ $\underline{q+B \rightarrow q(\rightarrow M+q)+B^*}$ $\underline{q+B \rightarrow M+q+B^*}$ $\underline{(qq)+B \rightarrow M+B^*+qq}$ $B+B \rightarrow M+B^*+B^*$	$(p_\perp^2)^{-6}\epsilon^5$ $(p_\perp^2)^{-6}\epsilon^5$ $(p_\perp^2)^{-8}\epsilon^3$ $(p_\perp^2)^{-10}\epsilon^1$ $(p_\perp^2)^{-12}\epsilon^{-1}$
	$B+B \rightarrow M+M^*+B^*+B^* \quad (n=16)$	$\underline{M+q \rightarrow M+q}$ $\underline{q+q \rightarrow \bar{q}(\rightarrow M+\bar{q})+B^*}$ $\underline{q+q \rightarrow M+B^*+\bar{q}}$ $M+B \rightarrow M+B^*$	$(p_\perp^2)^{-4}\epsilon^9$ $(p_\perp^2)^{-4}\epsilon^9$ $(p_\perp^2)^{-6}\epsilon^7$ $(p_\perp^2)^{-8}\epsilon^5$
	$B+B \rightarrow M+M^*+M^*+B^*+B^* \quad (n=18)$	$\underline{q+\bar{q} \rightarrow M+M^*}$ $\underline{q+M \rightarrow q(\rightarrow M+q)+M^*}$	$(p_\perp^2)^{-4}\epsilon^{11}$ $(p_\perp^2)^{-4}\epsilon^{11}$
$B+B \rightarrow \bar{B}+X$	$B+B \rightarrow \bar{B}+B^*+B^*+\bar{B}^* \quad (n=18)$	$\underline{q+q \rightarrow B^*+\bar{q}(\rightarrow \bar{B}+qq)}$ $\underline{q+q \rightarrow B^*+\bar{B}+qq}$ $\underline{q+(qq) \rightarrow \bar{B}+B^*+B^*}$	$(p_\perp^2)^{-4}\epsilon^{11}$ $(p_\perp^2)^{-8}\epsilon^7$ $(p_\perp^2)^{-10}\epsilon^5$

RECENT DEVELOPMENTS IN THE THEORY OF
LARGE TRANSVERSE MOMENTUM PROCESSES*

TABLE I

Scaling Predictions for $E \, d\sigma/d^3p = C \, p_T^{-n} (1-x_T)^F$

Large p_T Process	Leading CIM Subprocess	Predicted	Observed (CP) [‡]
		n/F	n/F
$pp \rightarrow \pi^+ X$	$qM \rightarrow q\pi^+$	8//9	8.5//8.8
π^-	$qM \rightarrow q\pi^-$	8//9	8.9//9.7
K^+	$qM \rightarrow qK^+$	8//9	8.4//8.8
K^-	$qM \rightarrow qK^-$	8//13	8.9//11.7
	$q\bar{q} \rightarrow K^+ K^-$	8//11	
$pp \rightarrow pX$	$q(qq) \rightarrow Mp$	12//5	11.7//6.8
	$qB \rightarrow qp$	12//7	
$pp \rightarrow \bar{p}X$	$q\bar{q} \rightarrow B\bar{p}$	12//11	8.8//14.2
	$qM \rightarrow qM$	8//15	
$\pi p \rightarrow \pi X$	$q\bar{q} \rightarrow M\pi$	8//5	
	$qM \rightarrow q\pi$	8//7	
	$q(qq) \rightarrow B\pi$	12//3	
	$\pi q \rightarrow \pi q$	8//3	

Unified description of inclusive and exclusive reactions at all momentum transfers*

Comparison of 20 exclusive reactions at large t

TABLE I. Measured reactions presented in this paper. The reactions are written as (beam + target) \rightarrow (spectrometer particle + side particle). Reactions 1, 2, 3, 17, and 18 were measured with either final-state particle in the spectrometer.

Meson-baryon reactions	
1	$\pi^+ p \rightarrow p\pi^+$
2	$\pi^- p \rightarrow p\pi^-$
3	$K^+ p \rightarrow pK^+$
4	$K^- p \rightarrow pK^-$
5	$\pi^+ p \rightarrow p\rho^+$
6	$\pi^- p \rightarrow p\rho^-$
7	$K^+ p \rightarrow pK^{*+}$
8	$K^- p \rightarrow pK^{*-}$
9	$K^- p \rightarrow \pi^- \Sigma^+$
10	$K^- p \rightarrow \pi^+ \Sigma^-$
11	$K^- p \rightarrow \Lambda \pi^0$
12	$\pi^- p \rightarrow \Lambda K^0$
13	$\pi^+ p \rightarrow \pi^+ \Delta^+$
14	$\pi^- p \rightarrow \pi^- \Delta^+$
15	$\pi^- p \rightarrow \pi^+ \Delta^-$
16	$K^+ p \rightarrow K^+ \Delta^+$
Baryon-baryon reactions	
17	$pp \rightarrow pp$
18	$\bar{p}p \rightarrow p\bar{p}$
19	$\bar{p}p \rightarrow \pi^+ \pi^-$
20	$\bar{p}p \rightarrow K^+ K^-$

TABLE V. The scaling between E755 and E838 has been measured for eight meson-baryon and 2 baryon-baryon interactions at $\theta_{c.m.} = 90^\circ$. The nominal beam momentum was 5.9 GeV/c and 9.9 GeV/c for E838 and E755, respectively. There is also an overall systematic error of $\Delta n_{\text{sys}} = \pm 0.3$ from systematic errors of $\pm 13\%$ for E838 and $\pm 9\%$ for E755.

No.	Interaction	Cross section		$n-2$
		E838	E755	$(\frac{d\sigma}{dt} \sim 1/s^{n-2})$
1	$\pi^+ p \rightarrow p\pi^+$	132 ± 10	4.6 ± 0.3	6.7 ± 0.2
2	$\pi^- p \rightarrow p\pi^-$	73 ± 5	1.7 ± 0.2	7.5 ± 0.3
3	$K^+ p \rightarrow pK^+$	219 ± 30	3.4 ± 1.4	$8.3^{+0.6}_{-1.0}$
4	$K^- p \rightarrow pK^-$	18 ± 6	0.9 ± 0.9	≥ 3.9
5	$\pi^+ p \rightarrow p\rho^+$	214 ± 30	3.4 ± 0.7	8.3 ± 0.5
6	$\pi^- p \rightarrow p\rho^-$	99 ± 13	1.3 ± 0.6	8.7 ± 1.0
13	$\pi^+ p \rightarrow \pi^+ \Delta^+$	45 ± 10	2.0 ± 0.6	6.2 ± 0.8
15	$\pi^- p \rightarrow \pi^+ \Delta^-$	24 ± 5	≤ 0.12	≥ 10.1
17	$pp \rightarrow pp$	3300 ± 40	48 ± 5	9.1 ± 0.2
18	$\bar{p}p \rightarrow p\bar{p}$	75 ± 8	≤ 2.1	≥ 7.5

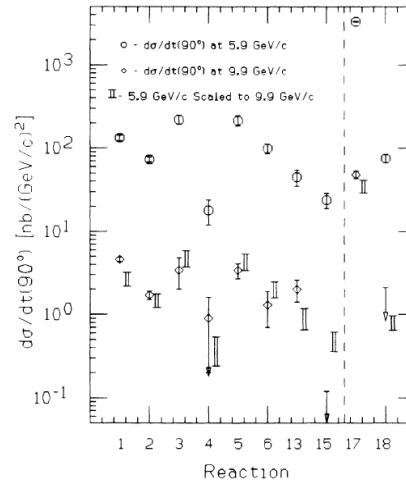


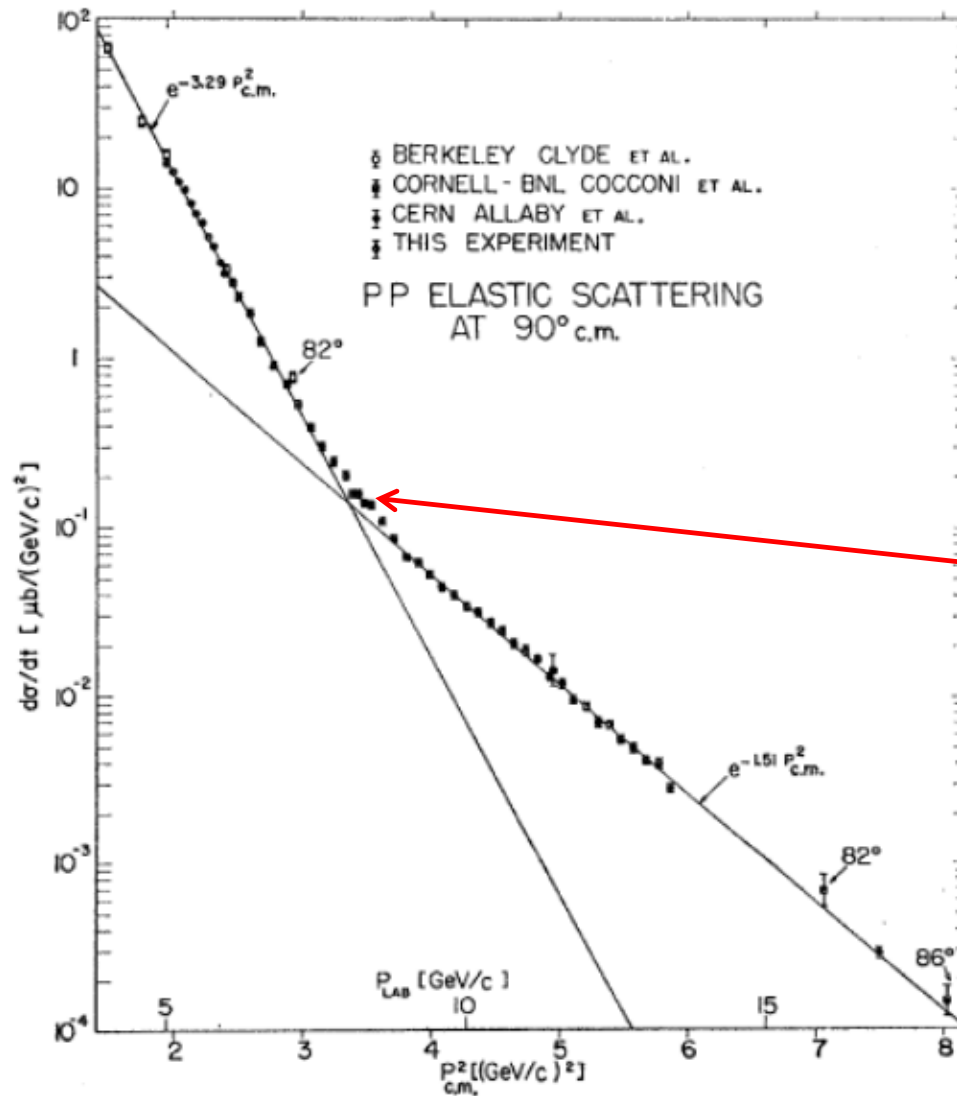
FIG. 26. The scaling between E755 and E838 has been calculated for eight meson-baryon and 2 baryon-baryon interactions at $\theta_{c.m.} = 90^\circ$. The beam momentum for E838 was 5.9 GeV/c, corresponding to $s = 11.9 \text{ GeV}^2$ for meson-baryon reactions and $s = 12.9 \text{ GeV}^2$ for baryon-baryon reactions. For the 9.9 GeV/c momentum of E755, the corresponding values of s are 19.6 and 20.5 GeV^2 .

Which the energy range is interesting?

**NN-interactions and SPIN problems
($p_T \sim 2$ GeV/c anomaly and
diquark nucleon component)**

pp \rightarrow pp (90°)

C.W. Akerlof et al., Phys.Rev., vol.159, N5, 1138-1149, 1967



Krisch A. and Leksin G. -
non pointlike structure
of nucleon

$p_T \sim 2 \text{ GeV}/c$

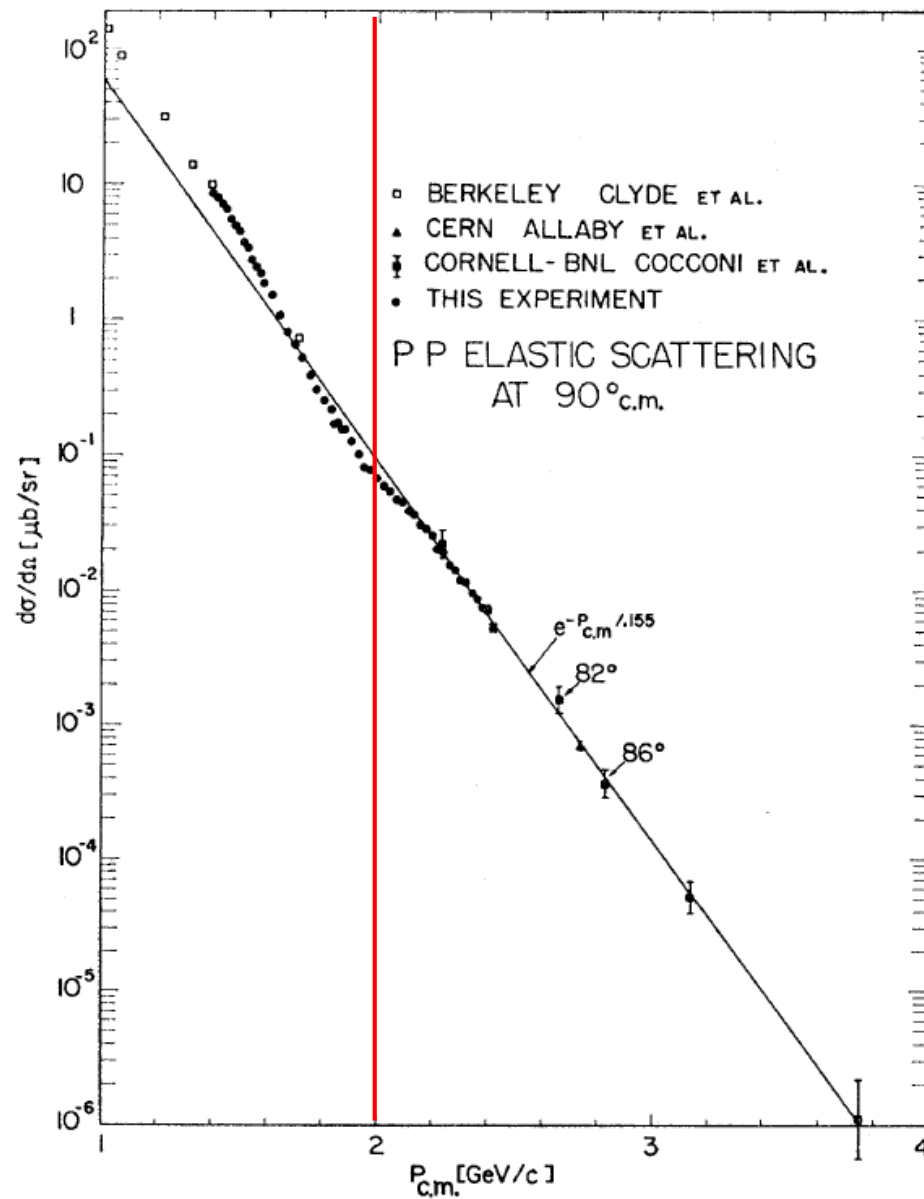
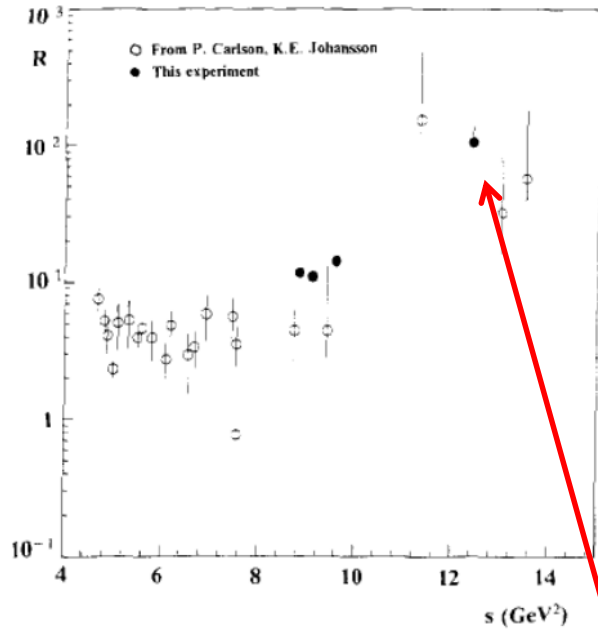


FIG. 9. Plot of $d\sigma/dt$ versus $\beta^2 P_1^2$ for all high-energy proton-proton elastic scattering. Other data (Refs. 13, 20, 22, 23), are also plotted. The lines drawn are straight line fits to the data.

$p\bar{p}$ 

$$R = \frac{\sigma(pp \rightarrow pp)}{\sigma(p\bar{p} \rightarrow p\bar{p})} (90^\circ \text{ c.m.})$$

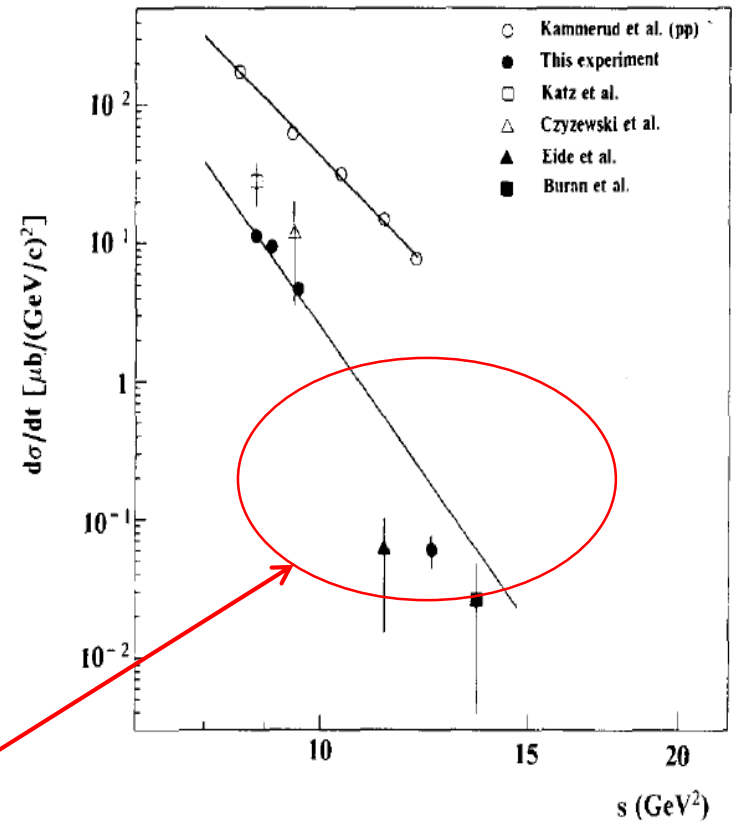
 $p_T \sim 2 \text{ GeV}/c \text{ region}$ 

Fig. 3. The $p\bar{p}$ and pp elastic differential cross sections at 90° CM as function of the square of the CM energy, s . Open circles are pp data from ref. [6]. These data fit well to the drawn curve proportional to s^{-9} . The remaining points are $p\bar{p}$ data. Shaded from this experiment. Otherwise from ref. [7] (open square), ref. [8] (open triangle) ref. [9] (shaded triangle) and ref. [10] (shaded square). The lower curve is an s^{-n} fit to four data points of this experiment, neglecting systematic errors. One obtains $n=12.3 \pm 0.2$, but evidently the data do not seem to follow this kind of a power law.

$p_T \sim 2 \text{ GeV}/c$ region

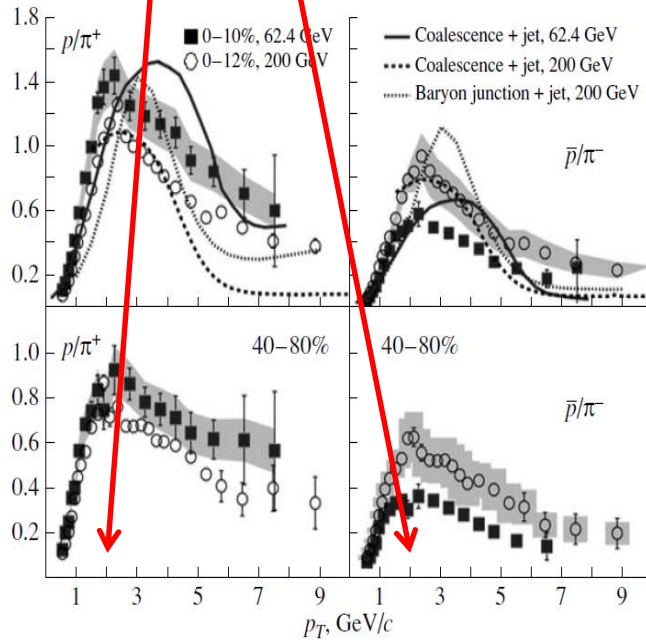


Fig. 3. [10] Ratio of the cross sections for the production of protons and charged pions as a function of the transverse momentum for various degrees of centrality and two beam energies of 62.4 and 200 GeV: (points) results of the STAR experiment and (curves) results of model calculations.

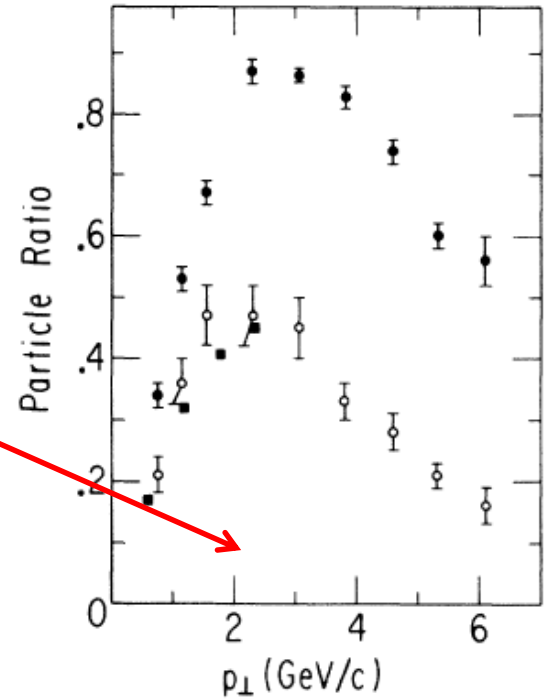
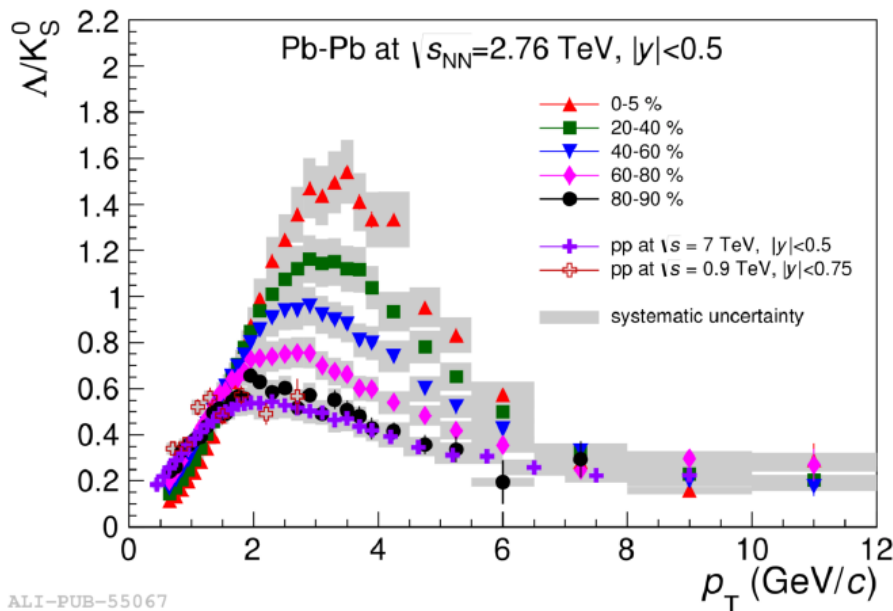
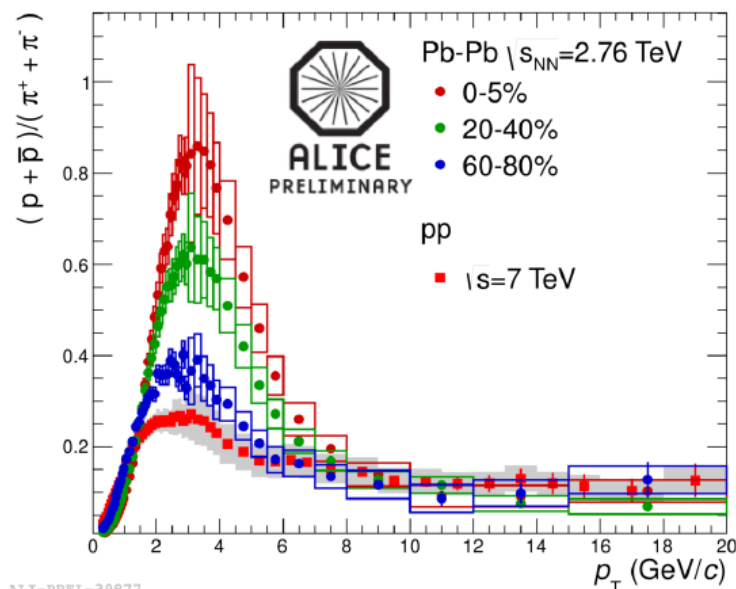


FIG. 20. Comparison of the cross-section ratio p/π^+ measured on tungsten at $\sqrt{s}=23.7 \text{ GeV}$ (closed circles), with that obtained by extrapolation to $A=1$ (open circles). Ratios obtained from the British-Scandinavian collaboration (Ref. 23) at $\sqrt{s}=23.4 \text{ GeV}$ are also plotted (closed squares).

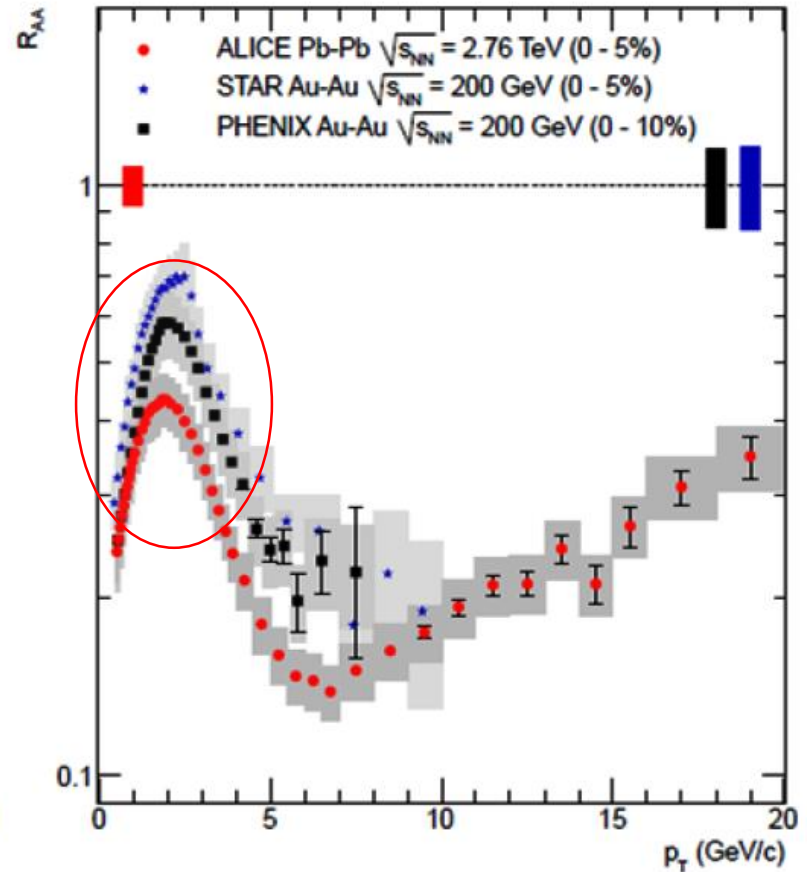
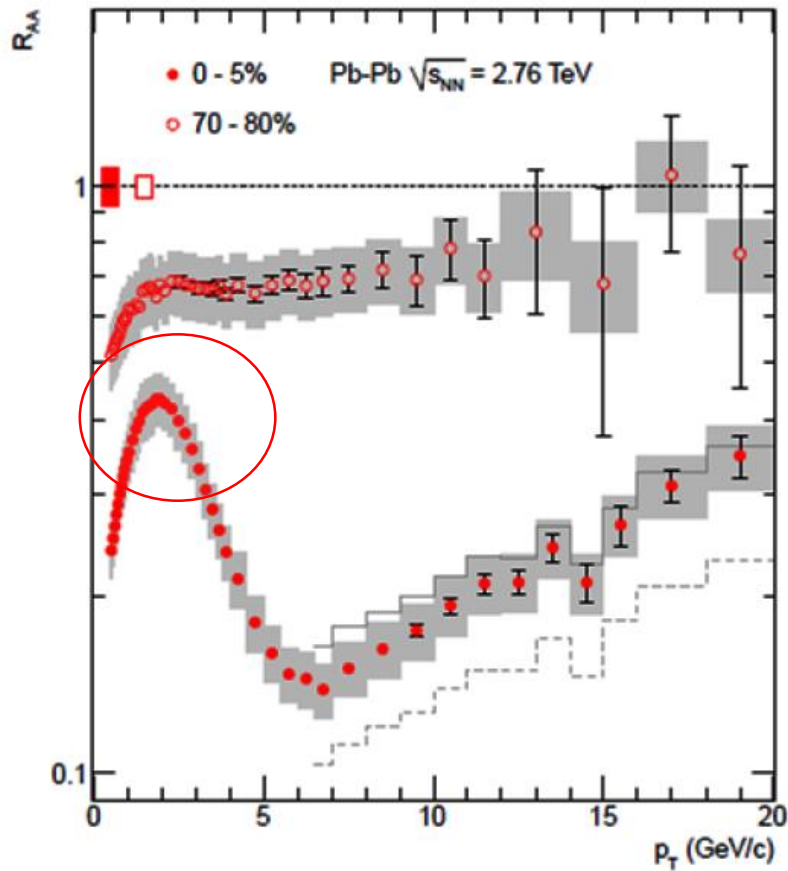


Baryon anomaly in Pb-Pb



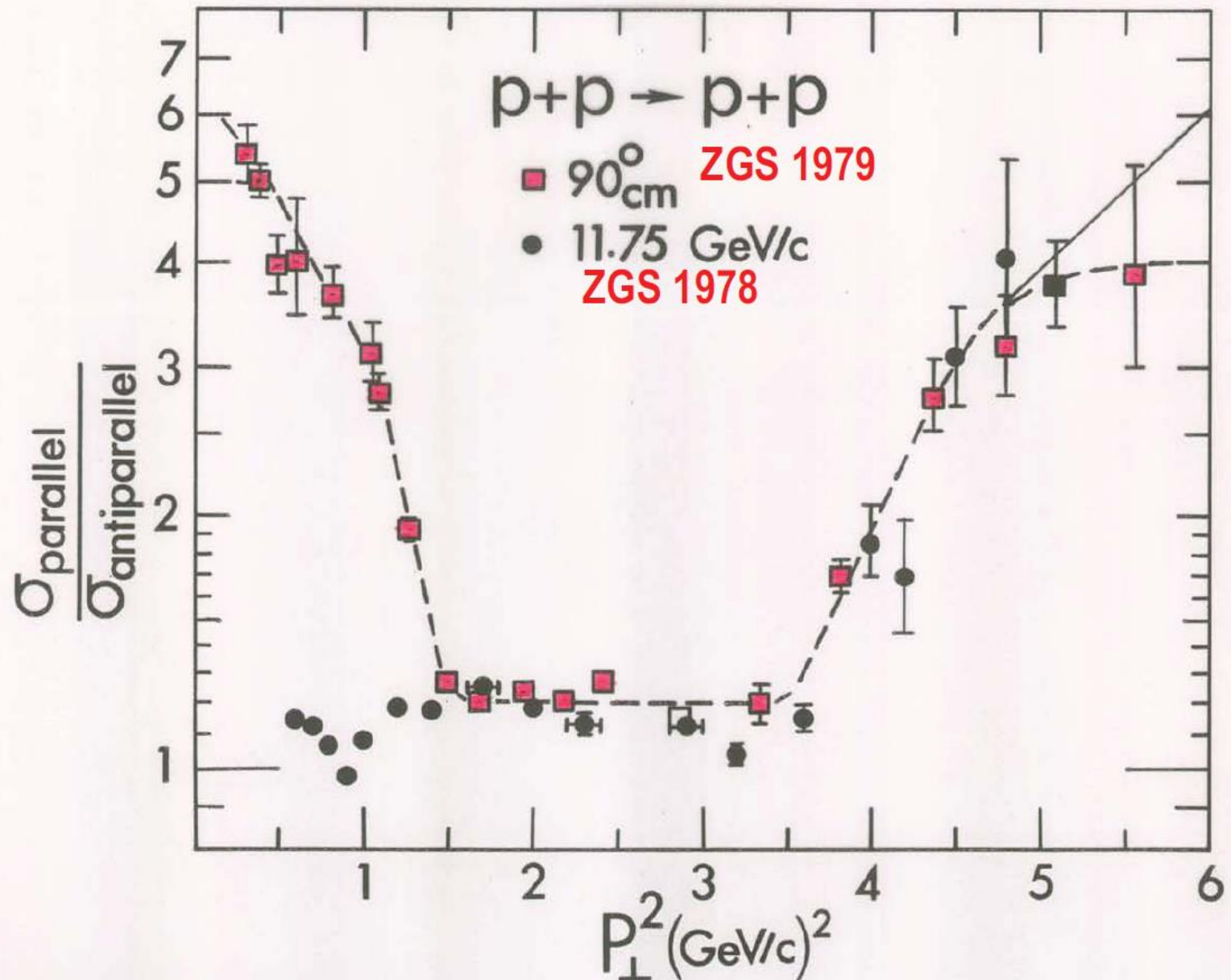
- Baryon to meson ratio increasing with centrality for $p_T < 8$ GeV/c.
 - Enhancement at moderate p_T is consistent with radial flow
 - May be explained by quark recombination from QGP (coalescence model)
- For $p_T > 8$ GeV/c no dependence on centrality and collision system
 - Consistent with fragmentation in vacuum

$p_T \sim 2$ GeV/c anomaly at high energy (RHIC and LHC)



SPIN physics and isotopic problem

Answer to Questions by Profs. Weisskopf & Bethe



Spin-Spin Forces in 6-GeV/c Neutron-Proton Elastic Scattering

D. G. Crabb, P. H. Hansen, A. D. Krisch, T. Shima, and K. M. Terwilliger
Randall Laboratory of Physics, The University of Michigan, Ann Arbor, Michigan 48109

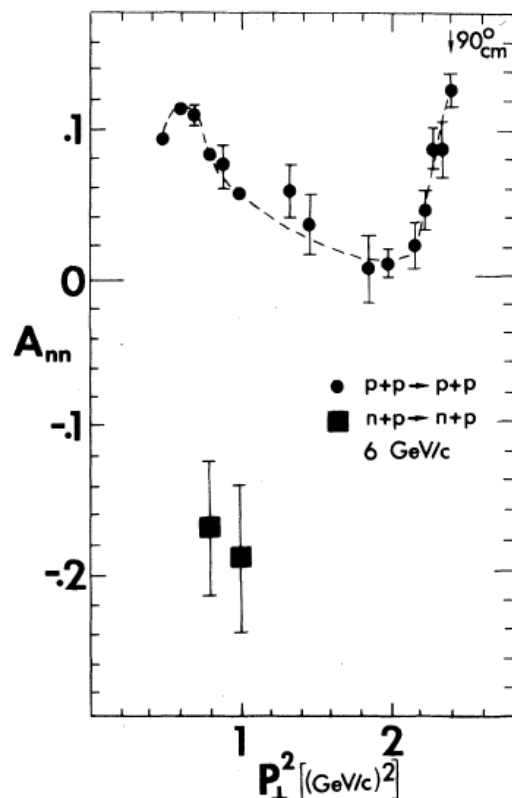


FIG. 2. The spin-spin correlation parameter, A_{nn} , for pure-initial-spin-state nucleon-nucleon elastic scattering at 6 GeV/c is plotted against the square of the transverse momentum. The proton-proton and neutron-proton data are quite different.

This large negative A_{nn} for n - p elastic scattering is quite unexpected. No theoretical models predicted this effect, although a very recent constituent-interchange model¹² predicts $A_{nn} = -44\%$. This may support the suggestion that large spin effects are related to the composite nature of the nucleon.^{12,13} An earlier Regge-model prediction¹⁴ is inconsistent with our data. It seems somewhat surprising that A_{nn} is so large at a P_{\perp}^2 of only 1 (GeV/c)².

¹²G. R. Farrar, S. Gottlieb, D. Sivers, and G. H. Thomas, Phys. Rev. D **20**, 202 (1979).

Exotic states and flavor universality

DIQUARK NUCLEON COMPONENT

Multiquark states have been discussed since the 1st page of the quark model

A SCHEMATIC MODEL OF BARYONS AND MESONS *

M. GELL-MANN

California Institute of Technology, Pasadena, California

Received 4 January 1964



If we assume that the strong interactions of baryons and mesons are correctly described in terms of the broken "eightfold way" ¹⁻³, we are tempted to look for some fundamental explanation of the situation. A highly promised approach is the purely dynamical "bootstrap" model for all the strongly interacting particles within which one may try to derive isotopic spin and strangeness conservation and broken eightfold symmetry from self-consistency alone ⁴. Of course, with only strong interactions, the orientation of the asymmetry in the unitary space cannot be specified; one hopes that in some way the selection of specific components of the F-spin by electromagnetism and the weak interactions determines the choice of isotopic spin and hypercharge directions.

Even if we consider the scattering amplitudes of strongly interacting particles on the mass shell only and treat the matrix elements of the weak, electromagnetic, and gravitational interactions by means

ber $n_t - n_{\bar{t}}$ would be zero for all known baryons and mesons. The most interesting example of such a model is one in which the triplet has spin $\frac{1}{2}$ and $z = -1$, so that the four particles d^- , s^- , u^0 and b^0 exhibit a parallel with the leptons.

A simpler and more elegant scheme can be constructed if we allow non-integral values for the charges. We can dispense entirely with the basic baryon b if we assign to the triplet t the following properties: spin $\frac{1}{2}$, $z = -\frac{1}{3}$, and baryon number $\frac{1}{3}$. We then refer to the members $u^{\frac{2}{3}}$, $d^{-\frac{1}{3}}$, and $s^{-\frac{1}{3}}$ of the triplet as "quarks" ⁶ q and the members of the anti-triplet as anti-quarks \bar{q} . Baryons can now be constructed from quarks by using the combinations (qqq) , $(qqq\bar{q}\bar{q})$, etc., while mesons are made out of $(q\bar{q})$, $(qq\bar{q}\bar{q})$, etc. It is assuming that the lowest baryon configuration (qqq) gives just the representations 1, 8, and 10 that have been observed, while the lowest meson configuration $(q\bar{q})$ similarly gives just 1 and 8.

that it would never have been detected. A search for stable quarks of charge $-\frac{1}{3}$ or $+\frac{2}{3}$ and/or stable di-quarks of charge $-\frac{2}{3}$ or $+\frac{1}{3}$ or $+\frac{4}{3}$ at the highest energy accelerators would help to reassure us of the non-existence of real quarks.

Status of the pentaquark problem

- 1st relatively certain **theoretical** suggestion
of mass ~ 1530 MeV and width < 15 MeV :
Diakonov, Petrov, Polyakov, Z.Phys., A359 (1997) 305.
- **Experiment** : about ten papers with **positive** evidences;
about ten papers with **negative** results
(some of them with higher statistics).
- **Common opinion and PDG position**
(since edition of 2008) :

Pentaquark is dead !

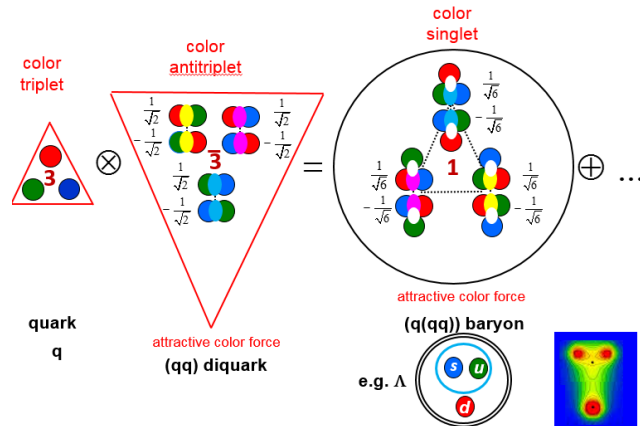
(Note, at the same time, great enthusiasm
in searches for tetraquarks !)

Hadrons from diquarks?

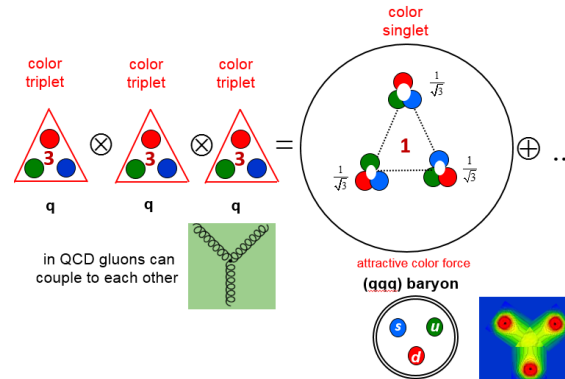
STATIC

Still an open question!

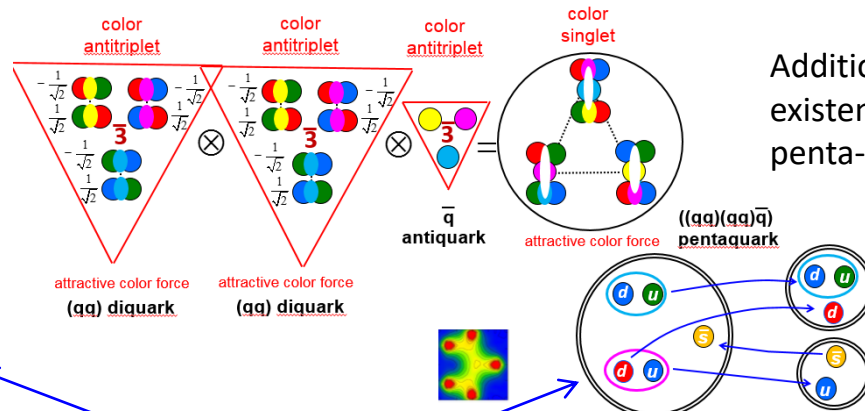
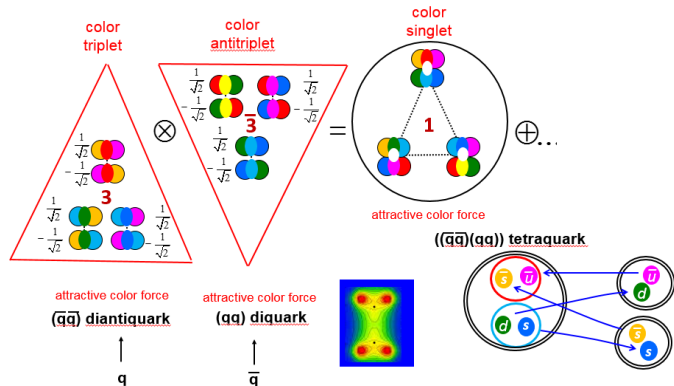
Role of diquarks in building hadrons?



VS.



Light and heavy baryon spectroscopy is sensitive to this question



Additional motivation for existence of tetra- and penta-quarks.

Exotic Hadrons, Dubna,
Sep.18,2018 Tomasz
Skwarnicki

Does effective mechanism to suppress rapid fall-apart exist?

**QUARK–DIQUARK SYSTEMATICS OF BARYONS:
SPECTRAL INTEGRAL EQUATIONS FOR SYSTEMS COMPOSED
BY LIGHT QUARKS**

© 2011 A. V. Anisovich, V. V. Anisovich*,

M. A. Matveev, V. A. Nikonov, A. V. Sarantsev, T. O. Vulfs

Petersburg Nuclear Physics Institute, Russian Academy of Sciences, Gatchina

Received May 7, 2010; in final form, August 30, 2010

How Often Do Diquarks Form? A Very Simple Model

Richard F. Lebed*

Department of Physics, Arizona State University, Tempe, Arizona 85287-1504, USA

(Dated: June, 2016)

Starting from a textbook result, the nearest-neighbor distribution of particles in an ideal gas, we develop estimates for the probability with which quarks q in a mixed q, \bar{q} gas are more strongly attracted to the nearest q , potentially forming a diquark, than to the nearest \bar{q} . Generic probabilities lie in the range of tens of percent, with values in the several percent range even under extreme assumptions favoring $q\bar{q}$ over qq attraction.

We have seen that the large relative size of the short-distance attraction between quarks in the color-antitriplet channel compared to the attraction between a quark and an antiquark in the color-singlet channel leads inexorably to a given quark being initially attracted to a quark rather than an antiquark a sizeable fraction of the time. We interpret this initial attraction as the seed event in the formation of a compact diquark qq rather than a color-singlet $q\bar{q}$ pair.

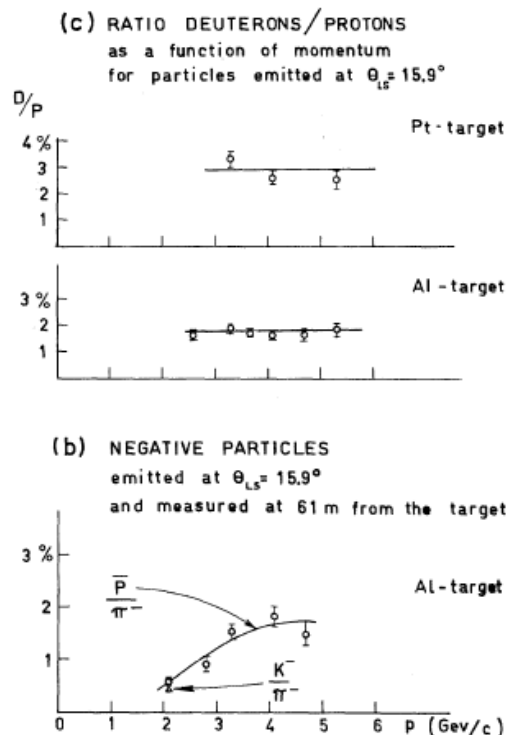
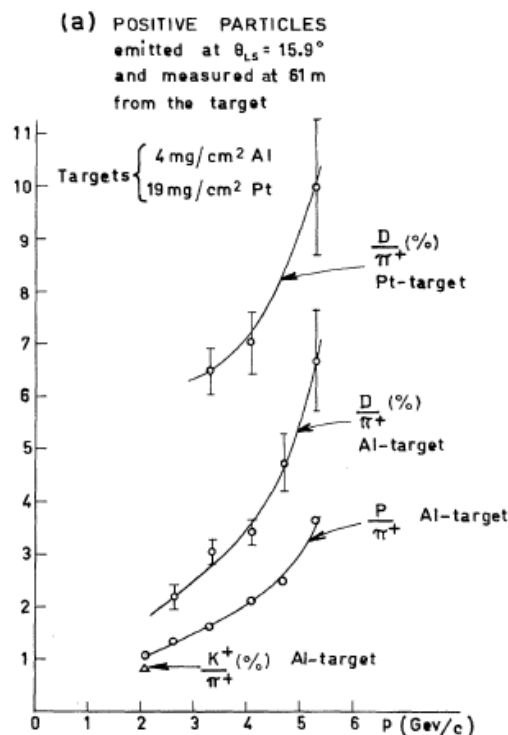
DIQURK DYNAMIC

MASS ANALYSIS OF THE SECONDARY PARTICLES PRODUCED BY THE 25-GEV PROTON BEAM OF THE CERN PROTON SYNCHROTRON

V. T. Cocconi,* T. Fazzini, G. Fidecaro, M. Legros,† N. H. Lipman, and A. W. Merrison
CERN, Geneva, Switzerland

(Received June 1, 1960)

We present here some results of a mass analysis of the secondary particles produced at 15.9° to the circulating beam in an aluminum target bombarded by 25-Gev protons in the CERN proton synchrotron.



Particle Production at Large Angles by 30- and 33-Bev Protons Incident on Aluminum and Beryllium*

V. L. FITCH, S. L. MEYER,† AND P. A. PIROUÉ

Palmer Physical Laboratory, Princeton University, Princeton, New Jersey

(Received February 12, 1962)

A mass analysis has been made of the relatively low momentum particles emitted from Al and Be targets when struck by 30- and 33-Bev protons. Measurements were made at 90°, 45°, and 131° relative to the direction of the Brookhaven AGS proton beam. Magnetic deflection and time-of-flight technique were used to determine the mass of the particles.

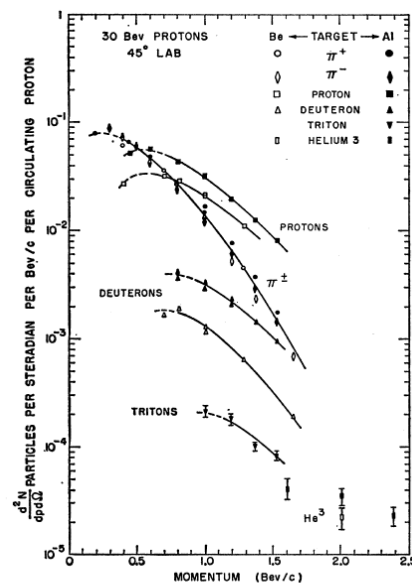


FIG. 3. Momentum spectra of particles emitted at 45° from aluminum and beryllium targets when struck by 30-Bev protons. Tritons from Be were not measured. For general remarks refer to Fig. 2 caption.

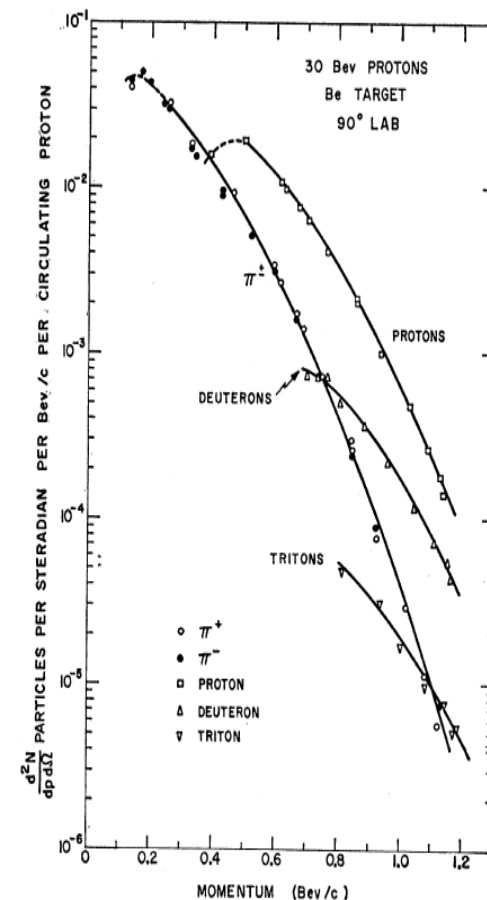
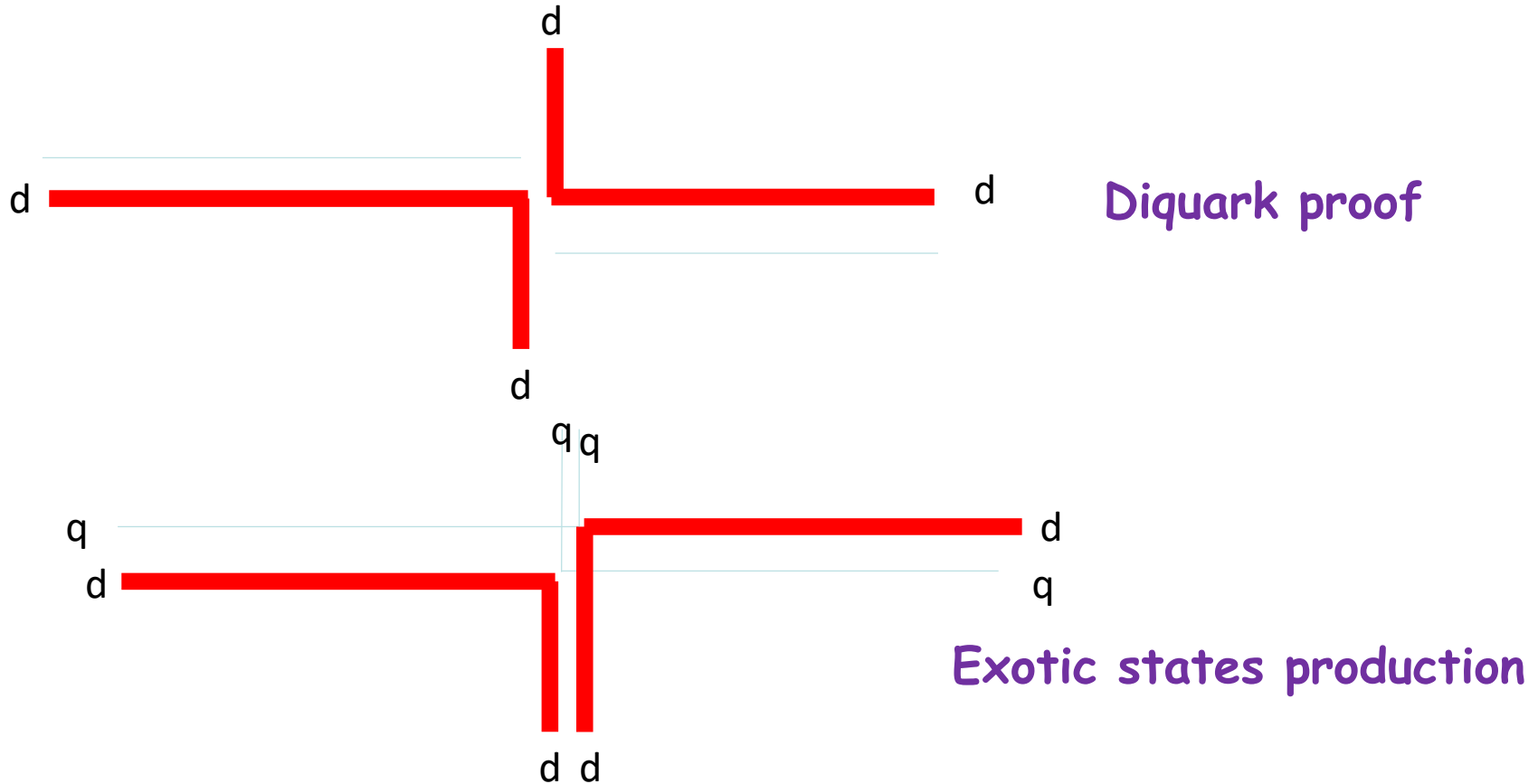


FIG. 2. Momentum spectrum of particles emitted at 90° from a beryllium target struck by 30-Bev protons. The ordinate is the number of particles produced at the target per steradian per Bev/c per circulating proton. The dashed portions of the curves indicate regions where the corrections due to multiple scattering exceed 15%. At the time these data were taken no effort was made to detect He³.

$pp \rightarrow pp + X, pp \rightarrow D + X$ reactions with diquarks



Kim's mechanisms

arXiv:1007.4705v5 [hep-ph] 25 Sep 2010
&Phys.Rev. C83 (2011) 054606
Carlos Granados and Misak Sargsian

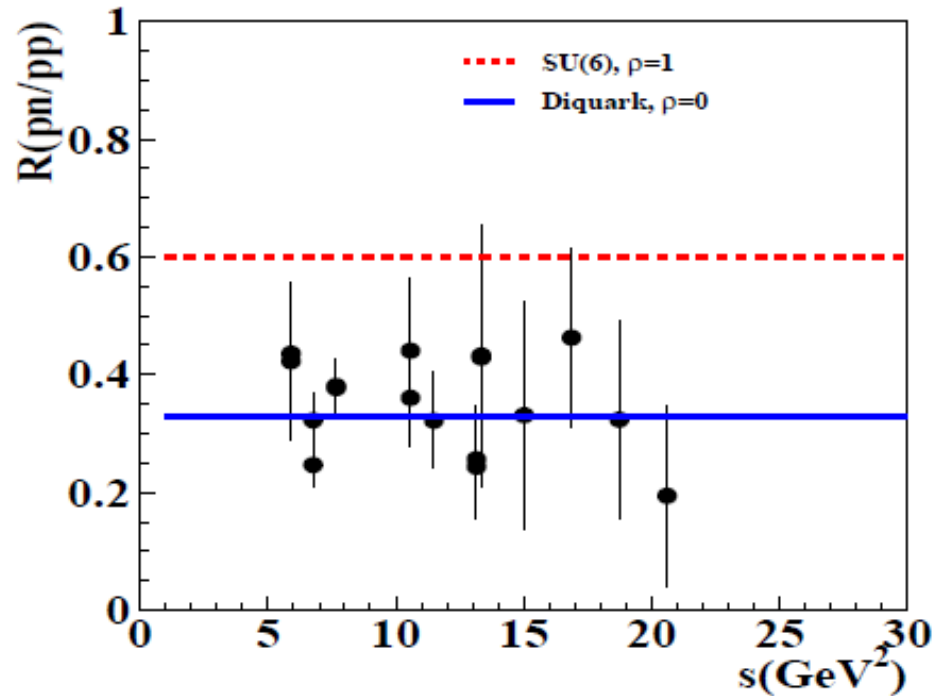


FIG. 2: (Color online) Ratio of the $pn \rightarrow pn$ to $pp \rightarrow pp$ elastic differential cross sections as a function of s at $\theta_{c.m.}^N = 90^\circ$.



How can we prove the existence
of diquarks and isotopic symmetry violation?

ELECTROMAGNETIC HADRON MASS DIFFERENCES AND ESTIMATION OF ISOTOPIC SYMMETRY VIOLATION PARAMETERS OF QCD VACUUM FROM QUARK MODEL.

A. E. DOROKHOV ¹

Joint Institute for Nuclear Research

Search for variation of fundamental constants and violations of fundamental symmetries using isotope comparisons

J. C. Berengut, V. V. Flambaum, and E. M. Kava

School of Physics, University of New South Wales, Sydney, NSW 2052, Australia

(Dated: 9 September 2011)

Atomic microwave clocks based on hyperfine transitions, such as the caesium standard, tick with a frequency that is proportional to the magnetic moment of the nucleus. This magnetic moment varies strongly between isotopes of the same atom, while all atomic electron parameters remain the same. Therefore the comparison of two microwave clocks based on different isotopes of the same atom can be used to constrain variation of fundamental constants. In this paper we calculate the neutron and proton contributions to the nuclear magnetic moments, as well as their sensitivity to any potential quark mass variation, in a number of isotopes of experimental interest including ^{201,199}Hg and ^{87,85}Rb, where experiments are underway. We also include a brief treatment of the dependence of the hyperfine transitions to variation in nuclear radius, which in turn is proportional to any change in quark mass. Our calculations of expectation-values of proton and neutron spin in nuclei are also needed to interpret measurements of violations of fundamental symmetries.

The estimations of the light quark mass differences, $m_d - m_u$, and the light quark condensate differences, $\langle \bar{D}D \rangle - \langle \bar{U}U \rangle$, are obtained in the framework of the quark model with QCD vacuum induced quark interaction. We consider long - wave condensate and short - wave instanton contributions to the electromagnetic hadron mass differences and show that the latter significantly improve the results on baryon octet. The results are: $m_d - m_u \approx 3.5 \text{ MeV}$ and $\langle \bar{D}D \rangle - \langle \bar{U}U \rangle \approx -(0 \sim 3) \cdot 10^{-3} \langle \bar{U}U \rangle$.

Search for variation of fundamental constants and violations of fundamental symmetries using isotope comparisons

J. C. Berengut, V. V. Flambaum, and E. M. Kava

School of Physics, University of New South Wales, Sydney, NSW 2052, Australia

(Dated: 9 September 2011)

Atomic microwave clocks based on hyperfine transitions, such as the caesium standard, tick with a frequency that is proportional to the magnetic moment of the nucleus. This magnetic moment varies strongly between isotopes of the same atom, while all atomic electron parameters remain the same. Therefore the comparison of two microwave clocks based on different isotopes of the same atom can be used to constrain variation of fundamental constants. In this paper we calculate the neutron and proton contributions to the nuclear magnetic moments, as well as their sensitivity to any potential quark mass variation, in a number of isotopes of experimental interest including $^{201,199}\text{Hg}$ and $^{87,85}\text{Rb}$, where experiments are underway. We also include a brief treatment of the dependence of the hyperfine transitions to variation in nuclear radius, which in turn is proportional to any change in quark mass. Our calculations of expectation-values of proton and neutron spin in nuclei are also needed to interpret measurements of violations of fundamental symmetries.

ОБЗОРЫ АКТУАЛЬНЫХ ПРОБЛЕМ

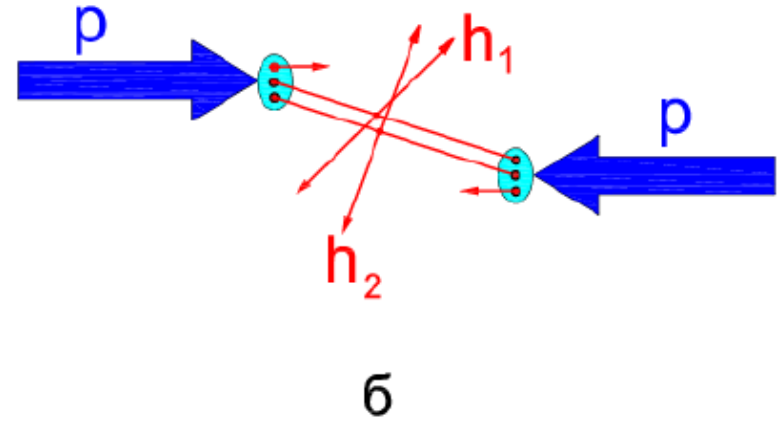
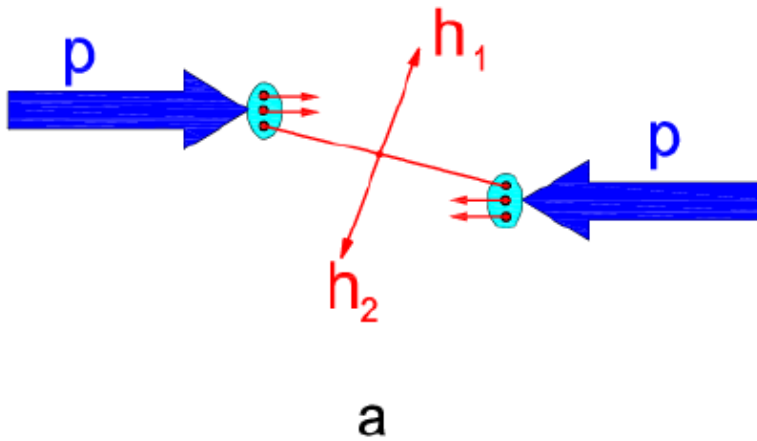
Сильное нарушение изотопической симметрии при рождении лёгких скалярных мезонов

Н.Н. Ачасов, Г.Н. Шестаков

Обсуждается нарушение изотопической симметрии как инструмента исследования механизмов рождения и природы лёгких скалярных мезонов. Речь идёт об эффектах нарушения изоспина, амплитуда которых $\sim \sqrt{m_d - m_u}$ (а не как обычно $\sim (m_d - m_u)$, где m_u и m_d — массы u - и d -кварков) и её модуль и фаза обладают характерной резонансной зависимостью от энергии в области $K\bar{K}$ -порогов. Рассмотрены разнообразные реакции, в которых может быть обнаружено или уже было обнаружено на опыте смешивание $a_0^0(980)$ - и $f_0(980)$ -резонансов, нарушающее изоспин из-за разницы масс K^+ - и K^0 -мезонов. Результаты экспериментов по поиску $a_0^0(980)$ - $f_0(980)$ -смешивания в распадах $f_1(1285) \rightarrow f_0(980)\pi^0 \rightarrow \pi^+\pi^-\pi^0$ и $\eta(1405) \rightarrow f_0(980)\pi^0 \rightarrow \pi^+\pi^-\pi^0$ подсказали более широкий взгляд на эффекты нарушения изотопической симметрии, обусловленные разностью масс K^+ - и K^0 -мезонов. Стало ясно, что подобные эффекты могут возникнуть не только вследствие $a_0^0(980)$ - $f_0(980)$ -смешивания, но и за счёт любого механизма рождения $K\bar{K}$ -пар с определённым изоспином в S -волне. Таким образом, появился новый инструмент для изучения механизмов рождения и природы лёгких скаляров. Особенно интересен случай большого нарушения изотопической симметрии в распаде $\eta(1405) \rightarrow f_0(980)\pi^0 \rightarrow \pi^+\pi^-\pi^0$ под действием механизма, содержащего аномальные пороги Ландау (логарифмические треугольные сингулярности), т.е. вследствие перехода $\eta(1405) \rightarrow (K^\bar{K} + \bar{K}^*K) \rightarrow (K^+K^- + K^0\bar{K}^0)\pi^0 \rightarrow f_0(980)\pi^0 \rightarrow \pi^+\pi^-\pi^0$. При этом принципиально важным оказывается учёт конечной ширины K^* -мезона.*

Way to resolve these problems

MPI and Exclusive reaction



Invariance Principles and Elementary Particles

PRINCETON UNIVERSITY PRESS
PRINCETON, NEW JERSEY
1964

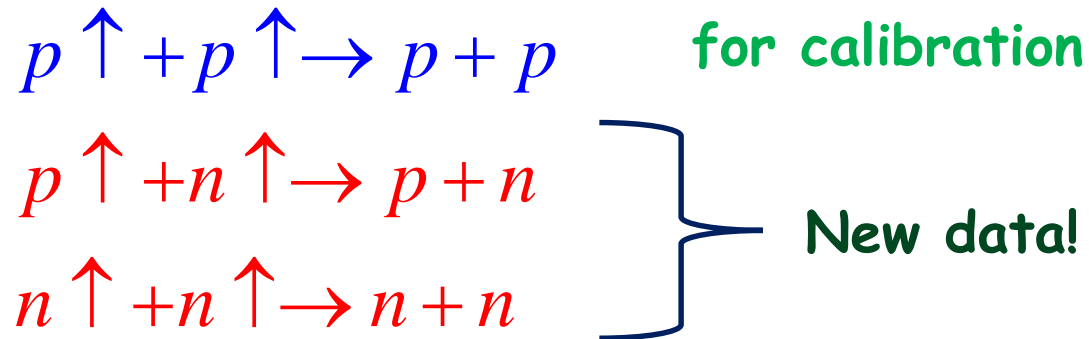
BY
J. J. SAKURAI

Isospin and Related Topics ($S = 0$)

9.1. History

The notion of isospin (or isotopic spin, isobaric spin, *i*-spin) was first introduced by Heisenberg (1932) as a convenient mathematical parameter to characterize the two charge states of what is now known as the nucleon. The nucleon is assumed to take isospin “up” ($T_3 = \frac{1}{2}$, proton) and isospin “down” ($T_3 = -\frac{1}{2}$, neutron) in analogy with the electron which can take ordinary spin “up” and ordinary spin “down.” This formalism is convenient because we know the algebra of spin $\frac{1}{2}$ systems from atomic physics.

NN Elastic scattering with polarized deuteron beams :



By the way we will have the counting rules verification!

pd, nd and dd - too!

Exclusive NN study at $x_T \sim 1$

$$N \uparrow + N \uparrow \rightarrow BB + MM$$

$$B(p, n, \Lambda, \Delta \dots), M(\pi, K, \dots)$$

Mechanisms of hyperons polarization

$$N \uparrow N \uparrow \rightarrow NN \quad \left\{ \begin{array}{l} \text{The counting rules and isotopic symmetry} \\ \text{studies, } p_T \sim 2 \text{ GeV}/c \text{ anomaly} \end{array} \right.$$

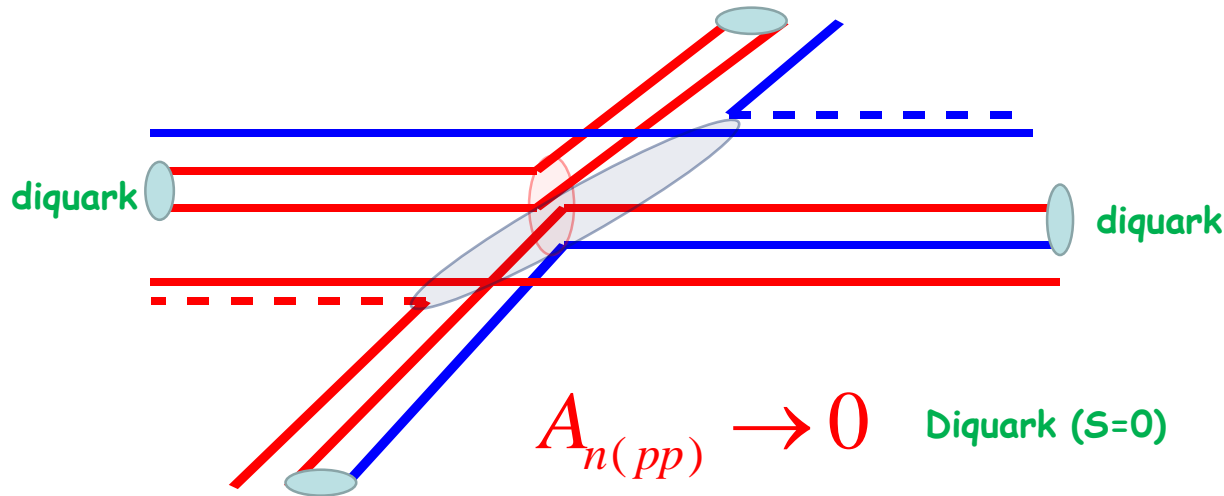
$$\begin{array}{l} N \uparrow N \uparrow \rightarrow BB + \pi\pi(KK) \\ N \uparrow N \uparrow \rightarrow \Delta\Delta \end{array} \quad \left\{ \right.$$

Detail vertexes studies
and spin structure of
the interaction vertex:

$$\begin{array}{l} q + (q) - (\text{quark} - \text{quark}) \\ q + (qq) - (\text{quark} - \text{diquark}) \\ (qq) + (qq) - (\text{diquark} - \text{diquark}) \end{array}$$

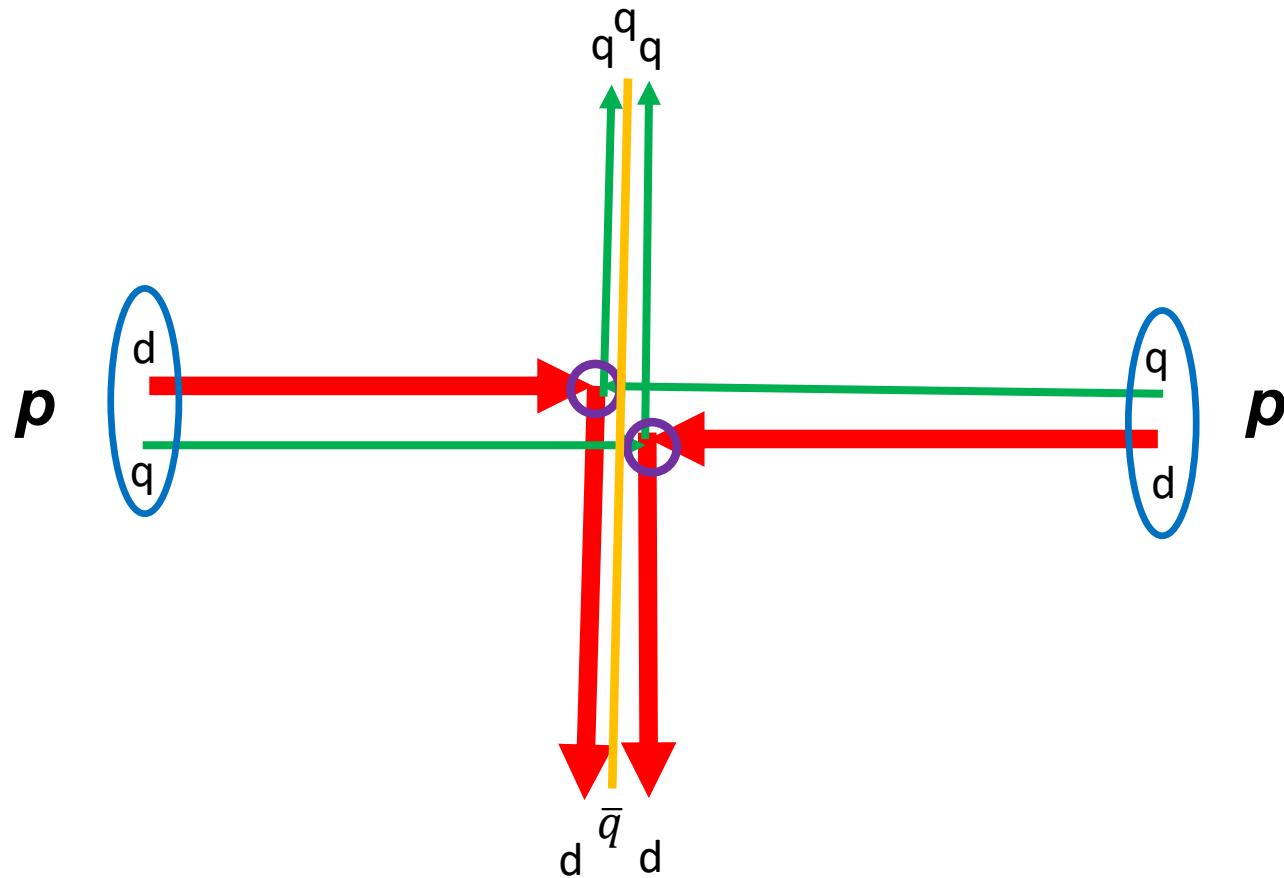
High p_T exclusive reactions -> MPI

$$\begin{array}{l}
 p \uparrow + p \uparrow \rightarrow B + B + M \bar{M} \\
 p \uparrow + p \uparrow \rightarrow p + p + \pi^0 \pi^0 (\pi^+ \pi^-)
 \end{array}
 \left\{
 \begin{array}{ll}
 R = \frac{N(\pi^+ \pi^-)}{N(\pi^0 \pi^0)} = \frac{2}{7} & \text{Without diquark} \\
 R = \frac{N(\pi^+ \pi^-)}{N(\pi^0 \pi^0)} \rightarrow 0 & \text{diquark}
 \end{array}
 \right.$$



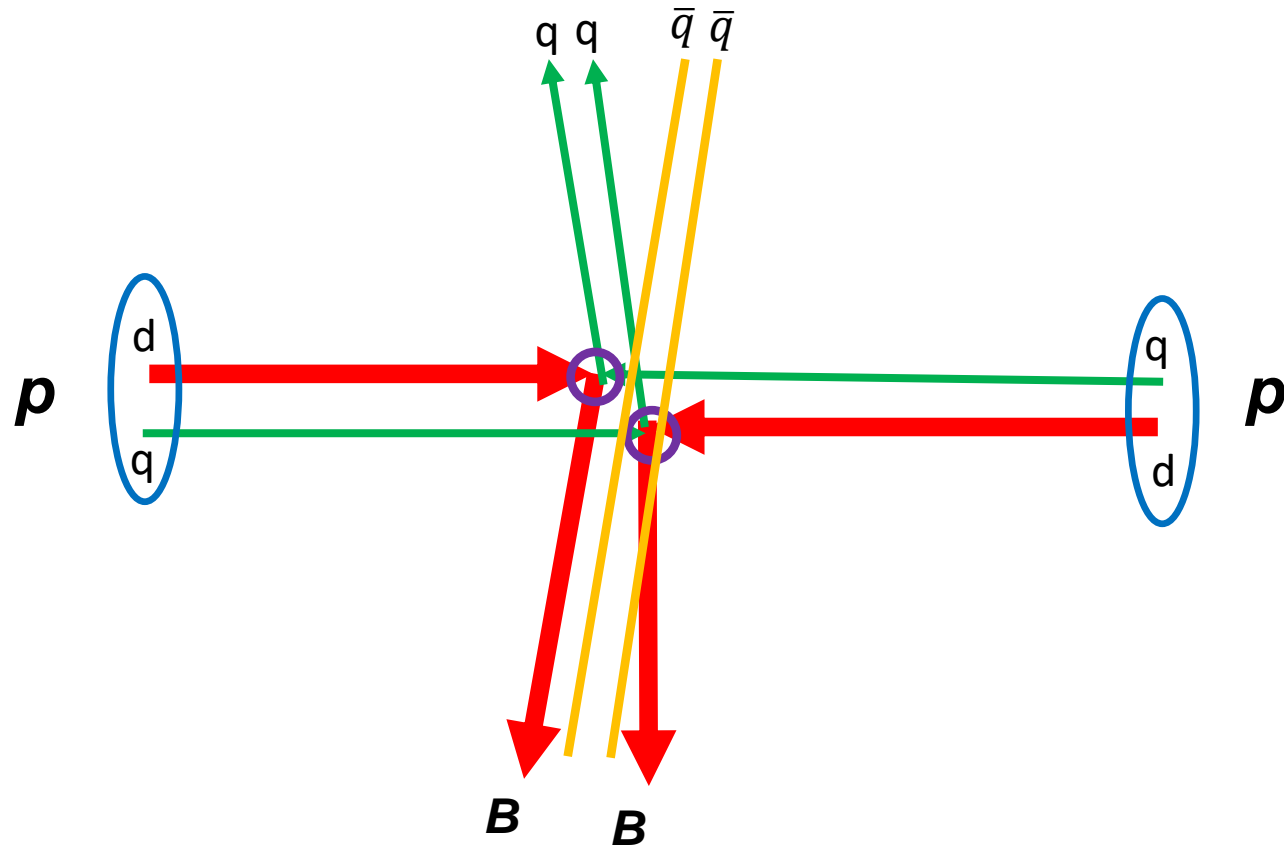
Exotic states production

pp - reactions with pentaquarks production

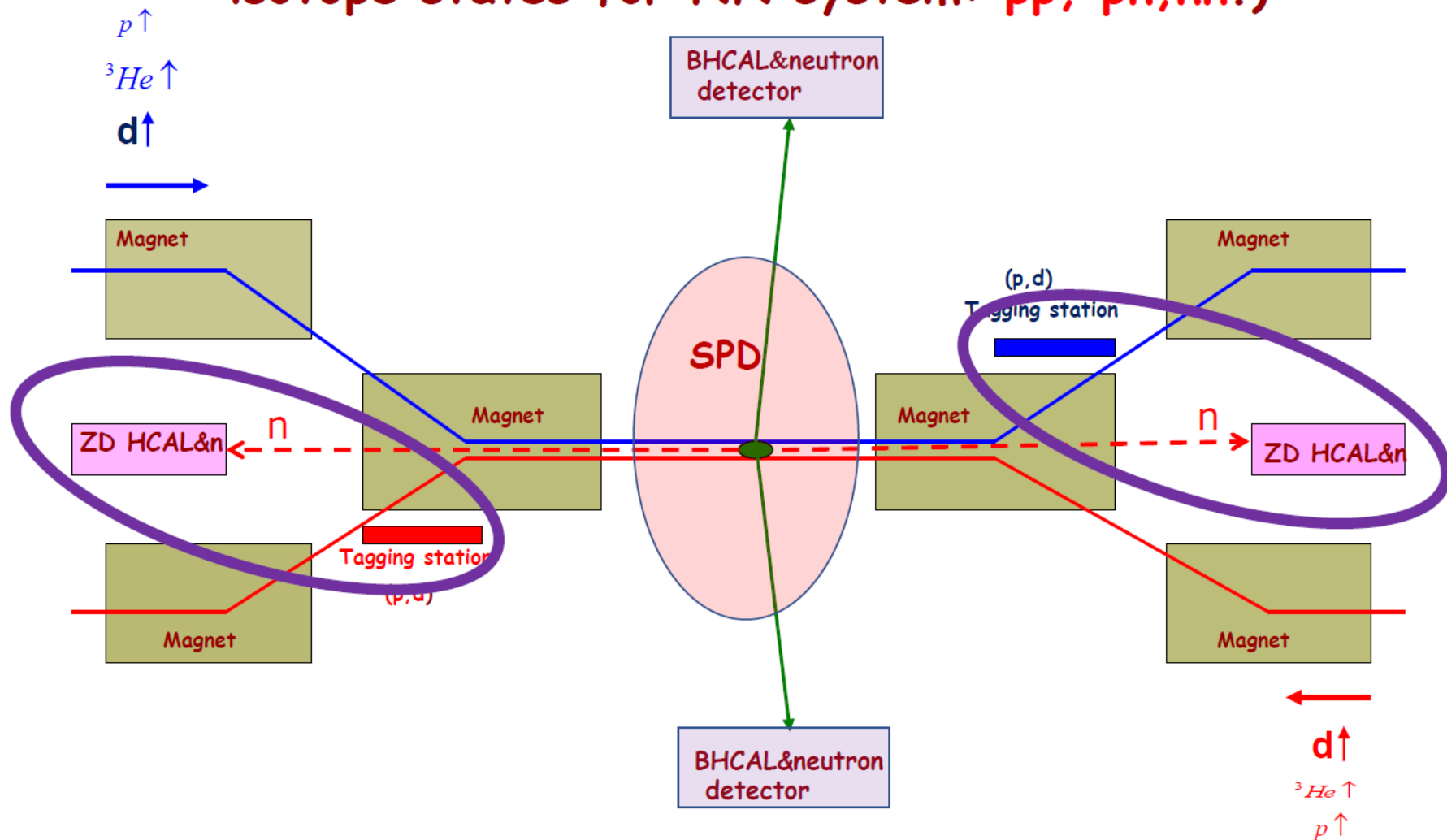


Exotic states production

pp - reactions with tetraquarks production



NICA Collision place for SPIN physics (deuteron and other beams, the first time all isotope states for NN system: pp , pn , nn .)



The tagging stations can be used as polarimeter!

END